Letter

Strong enhancements to superconducting properties of one-dimensional systems from metallic reservoirs

J. E. Ebot,[1,*] Sam Mardazad,[1] Lorenzo Pizzino,[2] Johannes S. Hofmann,[3,4] Thierry Giamarchi,[2] and Adrian Kantian[1,†]

[1]*SUPA, Institute of Photonics and Quantum Sciences, Heriot-Watt University, Edinburgh EH14 4AS, United Kingdom*

[2]*DQMP, University of Geneva, 24 Quai Ernest-Ansermet, 1211 Geneva, Switzerland*

[3]*Department of Condensed Matter Physics, Weizmann Institute of Science, Rehovot 76100, Israel*

[4]*Max-Planck-Institut für Physik komplexer Systeme, Nöthnitzer Strasse 38, 01187 Dresden, Germany*

(Received 28 July 2025; revised 1 March 2026; accepted 9 March 2026; published 7 April 2026)

Using an asymmetric two-leg ladder comprising pairing and metallic chains, this Letter proves the striking power of reservoir-mediated boosting of superconductivity. Using many-body numerics on large systems at zero and finite temperature, we unravel the processes by which the metal parameters can impact the effective pairing strength and the ranged pair-pair coupling mediated by the metal. These then enhance key superconducting properties far above those of the isolated system. Thus, our Letter identifies a general mechanism by which reservoirs can strongly suppress the effects of the Mermin-Wagner theorem in finite-sized systems, allowing even large one-dimensional systems to appear practically ordered.

DOI: 10.1103/1szk-xwh1

In the quest to engineer superconducting (SC) devices far beyond their current temperature limitations, one approach aims to boost the macroscopic phase coherence of electron pairs through the use of a metallic reservoir, while not degrading the strength of electron pair binding too much at the same time. The field arose from Kivelson's and Emery's work [1] on superconductivity emerging out of balancing two opposed goals: maximizing pair-phase coherence, which requires a low effective mass of the pairing mode, and maximizing pair-binding energy, which increases the mass of the pairing mode on a lattice. Theoretical and experimental work has aimed to show how electrons in one and two dimensions (1D and 2D) with intrinsic pairing could attempt to satisfy both goals at once, via coupling to a metallic reservoir [2–7]. For 2D systems, experiments on lanthanum strontium copper oxide (LSCO) and especially on FeSe monolayers atop reservoirs of itinerant electrons show striking enhancements to SC T_c over the isolated monolayer, but neither their cause nor their parametric dependence on reservoir properties is known [8,9]. To resolve these crucial questions and guide future experiments, theory studies simplified models, of a layer with an explicit pairing term (the P layer) in contact with a metallic one, modeled by free electrons (the M layer). Yet, no enhancement above the optimized T_c of the isolated 2D P layer could be demonstrated so far [3–6], though in the strong-pairing limit an improved T_c relative to the isolated baseline may have been described very recently [7]. However, the limited linear dimensions amenable to reliable numerics in 2D greatly constrain the possible parameter ranges for both P and M layers, preventing the study of those regimes most promising for boosting SC properties.

Moving to a 1D geometry allows to sidestep these constraints due to the available analytical and numerical control and understanding. In particular, these regimes were first explored analytically for a 1D P layer [10,11]. That work predicted that the metallic reservoir can boost the stiffness of the pair phase within the (1D) pairing chain (P chain) so strongly as to attain true SC ordering at zero temperature, due to the mediation of long-range coupling (low-exponent algebraic decay). Such long-range order in a 1D system arising from a microscopic model with purely short-range interactions would be extraordinary, and appears to strongly contradict the fundamental Mermin-Wagner theorem (MWT) that shows that no phase transition to any ordered state should be possible in such low-dimensional systems. To resolve these conflicting views requires nonperturbative, quantitatively reliable calculations on large systems. A crucial advantage of the 1D setting is then that numerics can treat systems of large linear extent, where any metal-mediated long-range coupling is expected to show the most pronounced enhancement to SC properties.

This Letter uses strong-coupling numerics to conclusively demonstrate the strong enhancement of superconductivity due to the metallic reservoir (M chain) in 1D hybrid systems [cf. Fig. 1(a)]. Joining P and M chains can drive SC susceptibilities *far above* those for the isolated P chain. Crucially, we show that even though the microscopic physics of P and M chains are strictly short ranged, it is possible to tune parameters over a broad range such as to strongly suppress the effects of the MWT, thus coming very close to the appearance of long-range order at both zero and finite temperatures even for large systems (cf. Figs. 2 and 3). We show that by tuning

*Contact author: je2011@hw.ac.uk
†Contact author: a.kantian@hw.ac.uk

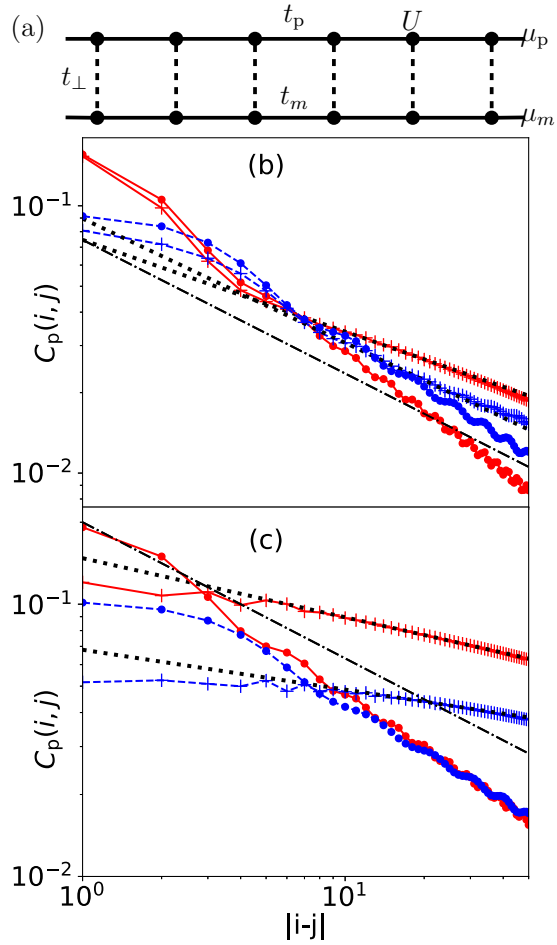

FIG. 1. (a) Overview of a two-leg ladder. (b) and (c) show C_p (see text) when k_F^p and k_F^m are comparable (red crosses) and far apart (blue crosses). Circles show C_p for an isolated P chain at matching densities. Dashed-dotted lines illustrate the slowest decay rate possible for the isolated P chain, at $K_p = 2$. Dotted lines show the power-law fit of C_p, with fitting parameters K_p^{-1} and $A_{C,p}$. (b) $U/t_p = 4$, $t_\perp/t_p = 0.4$. Red crosses show $k_F^p = 0.81$, $k_F^m = 1.02$, blue crosses show $k_F^p = 0.39$, $k_F^m = 1.44$. (c) $U/t_p = 10$, $t_m/t_p = 10$, $t_\perp/t_p = 3$. Red crosses show $k_F^p = 0.68$, $k_F^m = 0.89$, blue crosses show $k_F^p = 0.32$, $k_F^m = 1.24$.

either the nominal Fermi wave vectors of the two chains or the properties of the metal (or both), the effective pairing inside the P chain and the long-range coupling mediated by the metal, and finally the strength of long-range order can be tuned and optimized.

As shown in Fig. 1(a), we study a 1D attractive Hubbard model coupled to a 1D metallic bath, both with L sites (L even), with the Hamiltonian

$$\hat{H} = \sum_{i,\sigma,\lambda}^{L} -t_\lambda(\hat{c}^\dagger_{i,\sigma,\lambda}\hat{c}_{i+1,\sigma,\lambda} + \text{H.c.}) - \mu_\lambda \hat{n}_{i,\sigma,\lambda}$$
$$- t_\perp \sum_{i,\sigma}^{L}(\hat{c}^\dagger_{i,\sigma,\text{p}}\hat{c}_{i,\sigma,\text{m}} + \text{H.c.}) - U\sum_{i}^{L}\hat{n}_{i,\uparrow,\text{p}}\hat{n}_{i,\downarrow,\text{p}}, \quad (1)$$

where $\lambda = \text{p, m}$ indexes the P and M chain, respectively, and $\hat{c}_{i,\sigma,\lambda}$ is the fermionic annihilator for an electron at site i, of spin $\sigma = \pm 1/2$, in chain λ, and $\hat{n}_{i,\sigma,\lambda} = \hat{c}^\dagger_{i,\sigma,\lambda}\hat{c}_{i,\sigma,\lambda}$. The chains have separate chemical potentials μ_λ and tunneling t_λ, $U > 0$ parametrizes the strength of pairing in the isolated P

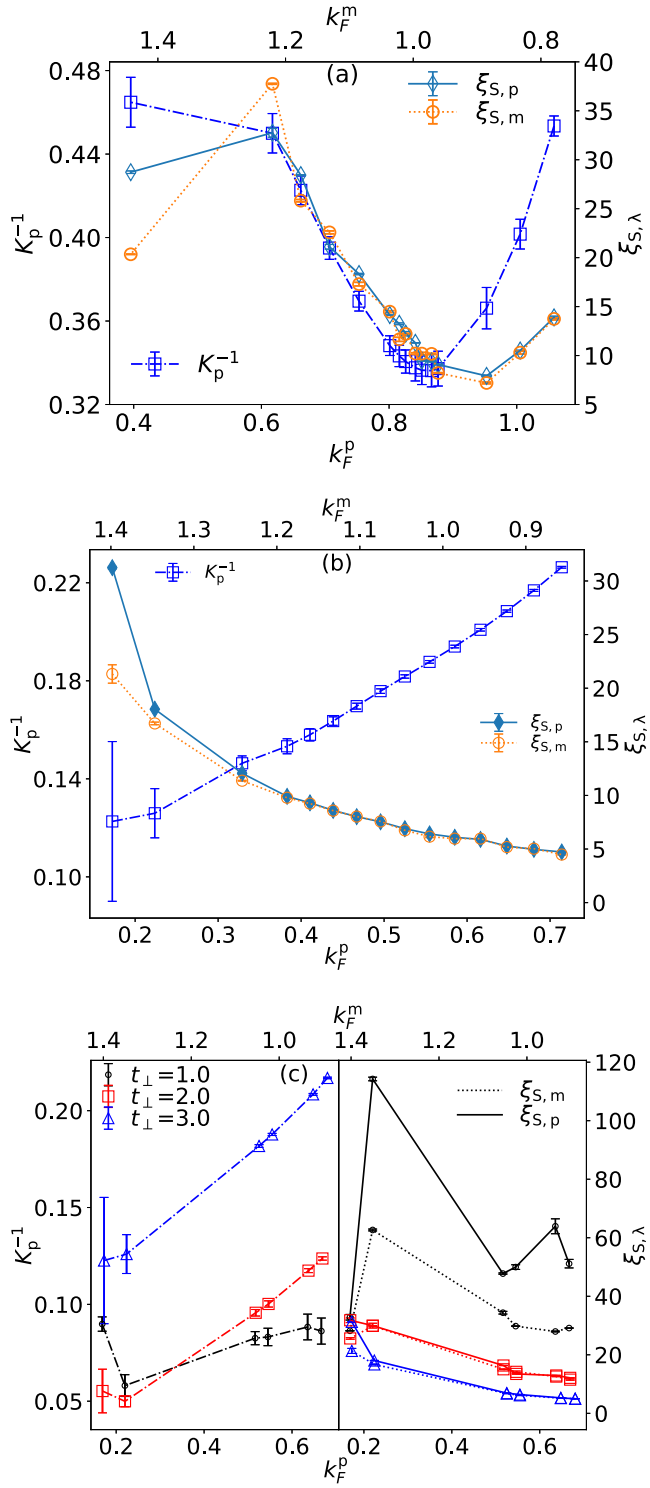

FIG. 2. Left y axis: K_p^{-1} vs k_F^p. Right y axis: $\xi_{S,p}$ and $\xi_{S,m}$ vs k_F^p. The top axis allows to read off the corresponding k_F^m values. K_p^{-1} and $\xi_{S,m}$ are obtained from fits to MPS-based calculations of Eqs. (5) and (6). (a) Regime 1. (b) Regime 2. (c) Regime 2 for $t_\perp/t_p = 1$ (black), $t_\perp/t_p = 2$ (red), $t_\perp/t_p = 3$ (blue).

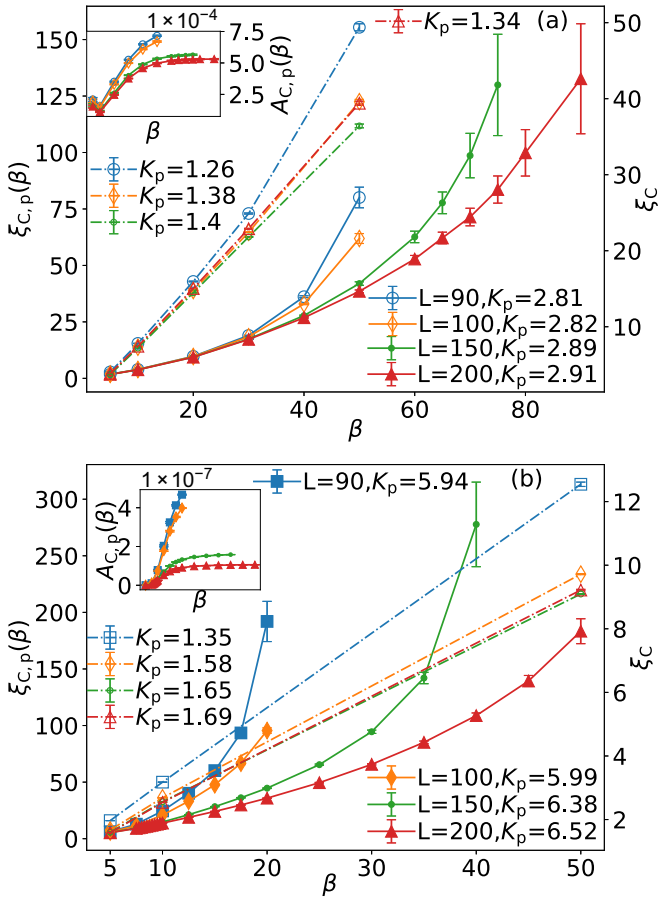

FIG. 3. Thermal SC correlation length $\xi_{C,p}$ (solid lines, left y axis) vs β at various L values, extracted from fitting AFQMC data. Insets show the corresponding fitted values of the nonuniversal amplitudes $A_{C,p}$. The values of K_p shown have been extracted from independent MPS-based calculations at $T = 0$. Where $\xi_{C,p}$ curves at different L collapse, superlinearity is evident relative to the isolated baseline ξ_C (dashed-dotted lines, right y axis). (a) Regime 1 at $k_F^p = 0.806$ and $k_F^m = 1.017$. (b) Regime 2 at $k_F^p = 0.3848$, $k_F^m = 1.1844$.

chain, and $t_\perp$ is the tunneling amplitude between the chains. We study this hybrid system when interchain coupling $t_\perp$ is smaller than the pairing gap

$$\Delta_p = \frac{1}{2}\left(\sum_\sigma E_{GS,p}(N+2\sigma,\sigma) - 2E_{GS,p}(N,0)\right), \quad (2)$$

where $E_{GS,p}(N, S_z)$ denotes the ground state energy of the isolated P chain with total charge N and z-spin S_z. We focus on two regimes, going up to $L = 200$; unless stated otherwise, all data shown are for $L = 200$ [12]:

$$\text{regime 1}: \; U/t_p = 4, \quad t_m/t_p = 1; \quad (3)$$

$$\text{regime 2}: \; U/t_p = 10, \quad t_m/t_p = 10. \quad (4)$$

Unless noted otherwise, we work at $t_\perp/t_p = 0.4$ in regime 1, and at $t_\perp/t_p = 3.0$ in regime 2. For regime 1, we find $\Delta_p/t_p \approx 0.69$, and for regime 2 it is $\Delta_p/t_p \approx 6.6$ across the studied range of densities. At temperature $T = 0$, we use the SYTEN package based on matrix product states (mps) [12,13], and at $T > 0$ the ALF package, based on auxiliary-field Quantum Monte Carlo (AFQMC) [12,14,15]. At $T = 0$, we thus drop μ_p and fix the global density of electrons n, to $n/2 = n_\uparrow = n_\downarrow = 0.58$ for regime 1, and to $n/2 = n_\uparrow = n_\downarrow = 0.5$ for regime 2, adjusting the relative densities in each chain via μ_m. We assign a nominal Fermi wave vector $k_F^\lambda = \pi n_\lambda/2$ to each chain, and by tuning μ_m we explore the impact of having nesting, $k_F^p \approx k_F^m$, compared against violating nesting to various degrees, $k_F^p \neq k_F^m$. At $T > 0$, where densities are only fixed on average, we then tune both μ_p and μ_m so as to work at specific densities. These are $n_p = 0.513$ and $n_m = 0.647$ for regime 1, and $n_p = 0.245$ and $n_m = 0.753$ for regime 2.

Regime 1 is the 1D analog to the basic setups studied previously in 2D, when tuning the properties of the metal to enhance superconductivity. Regime 2 has not previously been studied, and for 2D systems meaningful lattice sizes would not be possible anyway, due to the much smaller linear dimensions accessible to 2D numerics [5–7]. The purpose of regime 2 then is to maximally stabilize superconductivity in the P chain by using large values for both t_m and U. The large U value compensates for the weakening of effective pairing in the P chain due to the large t_m value (a reverse proximity effect). Viewed the other way around, the high t_m value aims at reducing the single-particle gap induced in the metal by the P chain (proximity effect) [12]. This unavoidable gap fundamentally changes the pair-pair coupling that the metal can mediate within the P chain: in previous perturbative analytical treatments, a single-particle correlator $\langle \hat{c}^\dagger_{i,\sigma,m}(\tau)\hat{c}_{j,\sigma,m}(0)\rangle$ with algebraic decay in either space or imaginary time would mediate long-range pair-pair coupling within the P chain which allows the system to sidestep the MWT and can thus lead to a 1D state with full SC order [11]. Our nonperturbative numerics show that this analysis neglects the crucial impact of the proximity effect on the M chain [12]. The resulting gap for single-particle excitations causes the metal to mediate exponentially decaying pair-pair coupling in the P chain instead, which thus does not escape the MWT. Still, this coupling can lead to a SC susceptibility enhanced to be far above the isolated P chain. In particular, increasing t_m as done in regime 2 yields a longer-ranged pair-pair coupling within the confines of exponential decay, resulting in strong improvements to SC susceptibilities.

For both chains, we analyze the s-wave pair-pair and single-particle correlation functions, respectively:

$$C_\lambda(i,j) = \langle \hat{c}^\dagger_{i,\uparrow,\lambda}\hat{c}^\dagger_{i,\downarrow,\lambda}\hat{c}_{j,\downarrow,\lambda}\hat{c}_{j,\uparrow,\lambda}\rangle, \quad (5)$$

$$S_\lambda(i,j) = \langle \hat{c}^\dagger_{i,\uparrow,\lambda}\hat{c}_{j,\uparrow,\lambda}\rangle. \quad (6)$$

We find that the decay of $C_\lambda(i,j)$ can be fitted with $(\pi A_{C,\lambda}(\beta)/\{\xi_{C,\lambda}(\beta)\sinh[\pi|i-j|/\xi_{C,\lambda}(\beta)]\})^{K_\lambda^{-1}}$, with $\beta = T^{-1}$, similar to the isolated Hubbard chain [16], but the amplitudes $A_{C,\lambda}$ are now temperature dependent (see below). The parameter K_λ is a Tomonaga-Luttinger-liquid (TLL) parameter that encodes the interactions and controls the SC susceptibility, which algebraically diverges with the power $K_\lambda^{-1} - 2$, as well as the finite-size condensate peak at zero momentum, which scales as $L^{1-K_\lambda^{-1}}$ [16]. As discussed above, for the maxima of S_λ we have to use the ansatz $A_{S,\lambda}e^{-|i-j|/\xi_{S,\lambda}}$ for *both* chains. The length scale $\xi_{S,m}$ encodes the effective

range of the pair-pair coupling induced in the P chain by the metal—the larger, the better the metal can stabilize the phase of pairs across the P chain [12]. Conversely, the length scale $\xi_{S,\mathrm{p}}$ encodes the effective strength of pairing in the P chain, which at $t_\perp > 0$ will depend not just on t_p, U, and μ_p, but on all parameters of the system—the larger $\xi_{S,\mathrm{p}}$, the weaker the effective pairing active within in the P chain. All fits are performed for distances up to $|i-j| = L/4$ in order to avoid boundary effects that become pronounced beyond this point, with i being one of the two central sites in each chain.

As illustrated in Figs. 1(b) and 1(c), both regimes can outperform the isolated Hubbard chain significantly, which is limited to $K_\mathrm{p}^{-1} > 1/2$ [16]. In fact, for the 1D hybrid systems we find $K_\mathrm{p}^{-1} < 1/2$ for all studied parameters (cf. Fig. 2). Especially regime 2 realizes remarkable enhancements to pair-pair correlations and thus K_p. Not only is K_p well above 2 in this regime, but it can be up to a factor of 4 larger than the K_p of the isolated P chain at comparable densities. We also note that we even find values of K_p much higher than the theoretical optimum of $K_{\rho,+} = 4$ for the symmetric charge mode of two weakly coupled identical chains which both have pairing. Especially, the high K_p values achievable in regime 2 will cause any observable, such as condensate peaks, to scale as barely distinguishable from an ordered SC state at the L values amenable to numerics.

Characterizing the ground states of our model across a wide range of relative densities $n_{\mathrm{p,m}}$ and thus Fermi wave vectors $k_F^{\mathrm{p,m}}$, a striking result is that we find $\xi_{S,\mathrm{p}} \approx \xi_{S,\mathrm{m}}$ almost across the board, as shown in Fig. 2. Thus, even in the regime where interchain tunneling $t_\perp$ is the weakest coupling scale and is well below Δ_p, both chains with their very different internal Hamiltonians still attempt aligning the correlation lengths associated with gapped single-electron excitations. However, in regime 2, when $k_F^\mathrm{p} \ll k_F^\mathrm{m}$ at $t_\perp/t_\mathrm{p} = 2.0, 3.0$, and throughout for $t_\perp/t_\mathrm{p} = 1.0$, the system does not succeed at aligning $\xi_{S,\mathrm{p}}$ and $\xi_{S,\mathrm{m}}$ [cf. Fig. 2(c)].

Even more striking is a mechanism for tuning system performance that is uncovered by the data in Fig. 2: controlling the positions of the wave vectors $k_F^{\mathrm{p,m}}$ relative to each other allows to optimize the SC susceptibilities of both regimes, i.e., to find the best possible balance between maximizing the range of pair-pair coupling, i.e., increasing $\xi_{S,\mathrm{m}}$, and maximizing pairing in the P chain, i.e., minimizing $\xi_{S,\mathrm{p}}$. For regime 1 [cf. Fig. 2(a)], where the mobility of pairs is already high in the isolated P chain, that optimal point sits close to, though not quite at, the nesting condition $k_F^\mathrm{p} = k_F^\mathrm{m}$. This minimizes the loss of pairing energy due to the reverse proximity effect, sitting near the minimum of the $\xi_{S,\mathrm{p}}(k_F^\mathrm{p})$ curve. Conversely, due to the high intrinsic mobility of pairs within the P chain, a low level of additional support stemming from the metal-mediated pair-pair coupling is sufficient to achieve the optimal SC susceptibility, with $\xi_{S,\mathrm{m}}$ sitting only a little above the minimum of the $\xi_{S,\mathrm{m}}(k_F^\mathrm{p})$ curve. For regime 2, the system improves its SC susceptibility in the opposite manner, by detuning k_F^p and k_F^m as much as possible, which increases $\xi_{S,\mathrm{p}}$ and $\xi_{S,\mathrm{m}}$, thus respectively depressing the strength of pairing and increasing the range of pair-pair coupling that the metal mediates in the P chain. With a low intrinsic pair mobility of the P chain due to the large U value, sacrificing pairing energy is a small price to pay in return for the strong enhancement to pair mobility afforded by an increasing $\xi_{S,\mathrm{m}}$ as k_F^p and k_F^m are tuned away from each other. In this way, tuning $k_F^{\mathrm{p,m}}$ and t_m allows each regime to get the most out of the metallic reservoir according to their specific needs. Lowering the value of $t_\perp$ from the default $t_\perp/t_\mathrm{p} = 3$ chosen for regime 2 indicates that tuning k_F^p could allow access to two different regimes, as shown in Fig. 2(c): at low k_F^p, the SC susceptibility peaks in between $t_\perp/t_\mathrm{p} = 1$ and $t_\perp/t_\mathrm{p} = 3$, while at higher k_F^p susceptibility decreases monotonically across the three $t_\perp/t_\mathrm{p}$ values studied. Moreover, at constant $t_\perp/t_\mathrm{p}$ the results summarized in Fig. 2(c) confirm our finding that the growing range of pair-pair coupling mediated by the metal, and weakening of pairing in the P chain, both caused by detuning k_F^p and k_F^m relative to each other, largely serves to improve SC susceptibility. Yet, we also find examples where this is not the optimal way, namely at low k_F^p and at intermediate $t_\perp/t_\mathrm{p} = 2$. Here, the system can only further lower K_p^{-1} by rebalancing in favor of a slightly strengthened pairing and reduced coupling range. The data in Fig. 2(c) further illustrate that the range of pair-pair coupling, as parametrized by $\xi_{S,\mathrm{m}}$, is not the only factor determining the efficacy of metal-induced stabilization of superconductivity. This is evidenced by the systems with higher $t_\perp$ often outperforming those with lower $t_\perp$ regarding SC susceptibility, even though these show much larger $\xi_{S,\mathrm{m}}$. This can be understood by looking at the leading order of the metal-mediated pair-pair coupling, which is controlled by a prefactor of $t_\perp^4/(\tilde{\Delta}_\mathrm{p} + \Delta_\mathrm{m})^2$ (cf. Ref. [11]), where $\tilde{\Delta}_\mathrm{p}$ denotes the renormalized pairing gap of the P chain, and Δ_m is the gap induced in the metallic chain by the proximity effect.

The strong boosts to the superconducting properties of the P chain by the metal show up at $T > 0$ as well, which is important for designing improved hybrid SC devices in practice. As shown in Fig. 3, we find that the thermal SC correlation length $\xi_{C,\mathrm{p}}(\beta)$ is not only far larger than for the isolated P chain, but also that when $\xi_{C,\mathrm{p}}$ curves at different L collapse, as they do for regime 1, they scale superlinearly in β. In contrast, the isolated P chain exhibits linear scaling in accordance with the predictions of conformal field theory. The only consistent way of obtaining $\xi_{C,\mathrm{p}}(\beta)$ from fits is to assume the nonuniversal amplitudes $A_{C,\mathrm{p}}$ to be temperature dependent, which they are not otherwise [16]. This expresses the fact that the form of any microscopic action derived for the P chain will depend on the state of the metal, which in turn will change with β. With $\xi_{C,\mathrm{p}}(\beta)$ boosted by more than an order of magnitude over that of the isolated P chain, with growing β the thermal SC correlation length rapidly matches and exceeds the central half of the system, i.e., that portion which exhibits bulk behavior undistorted by boundary effects and thus the region on which the fitting is performed. This manifests as an apparent onset of a divergence in $\xi_{C,\mathrm{p}}(\beta)$ once this length scale grows beyond roughly $L/4$, as the finite-size system becomes practically indistinguishable from its state at $T = 0$ from there on. In contrast to the isolated P chain, the size of our asymmetric two-leg ladder can thus be grown superlinearly with β and still appear to be entirely within the low- or zero-temperature regime.

This work demonstrates the powerful benefits to SC properties that can be derived from a metallic reservoir, and especially from tuning the parameters of the metal such as to deliberately promote mediated pair-pair coupling in

conjunction with the relative positions of the two chain's nominal Fermi surfaces. Our finding of reservoirs with short-range physics nevertheless being able to strongly abate the destructive effects of the MWT on ordering in low-dimensional correlated systems presents a powerful general approach to be translated to a large range of other systems, materials, and devices. It could, e.g., be applied to higher-dimensional analogs such as 2D bilayer systems [3–6] in which these effects—and their impact on the Berezinskii-Kosterlitz-Thouless (BKT) transition temperature—have not yet been explored on purpose, either experimentally or theoretically, but that would be especially important in the quest for a targeted design of high-T_c SC devices. Towards the latter, large-scale AFQMC-based simulations could be one possible approach, as would be continuous-time interaction expansion (CT-INT)-based QMC algorithms that integrate out the metal [17]. Furthermore, in the regime where tunneling in the y direction is weak in both layers, the recently developed matrix product states with mean-field (MPS + MF) technique for fermions [18] would make it possible to study far larger 2D bilayer systems than those amenable to any practical QMC-based simulations, and thus to probe regimes with large values of t_m/t_p and / or low U/t_p which might show exceptional enhancement to SC properties. Finally, ultracold atomic lattice gases present a physical platform where the basic models studied in this Letter—or its 2D variants—and the suppression of the MWT via reservoir, could be directly implemented and tested. Adapting strategies from the engineering of long-lived metastable states as theoretically proposed [19] and practically implemented [20] would allow to directly realize the types of 1D asymmetric two-leg ladders and 2D bilayer systems with a P and a M layer, and verify the physics revealed by the present work.

Acknowledgments. This work was supported by an ERC Starting Grant from the European Union's Horizon 2020 Research and Innovation Programme under Grant Agreement No. 758935, and the U.K.'s Engineering and Physical Sciences Research Council (EPSRC Grant No. EP/W022982/1). This work is also supported by the Swiss National Science Foundation under Grant No. 200020-219400. The computations were enabled by resources provided through multiple EPSRC "Access to HPC" calls on the ARCHER2, Peta4-Skylake and Cirrus compute clusters, as well as by computer time awarded by the National Academic Infrastructure for Supercomputing in Sweden (NAISS). This work was supported by a grant from the Swiss National Supercomputing Centre (CSCS) under Project ID s1307 on Alps. The authors also acknowledge the use of the HWU high-performance computing facility (DMOG) and associated support services in the completion of this work.

Data availability. The data that support the findings of this article are not publicly available upon publication because it is not technically feasible and/or the cost of preparing, depositing, and hosting the data would be prohibitive within the terms of this research project. The data are available from the authors upon reasonable request.

[1] V. J. Emery and S. A. Kivelson, Importance of phase fluctuations in superconductors with small superfluid density, Nature (London) **374**, 434 (1995).

[2] S. Kivelson, Making high T_c higher: a theoretical proposal, Physica B **318**, 61 (2002).

[3] E. Berg, D. Orgad, and S. A. Kivelson, Route to high-temperature superconductivity in composite systems, Phys. Rev. B **78**, 094509 (2008).

[4] G. Wachtel, A. Bar-Yaacov, and D. Orgad, Superfluid stiffness renormalization and critical temperature enhancement in a composite superconductor, Phys. Rev. B **86**, 134531 (2012).

[5] A. Zujev, R. T. Scalettar, G. G. Batrouni, and P. Sengupta, Pairing correlations in the two-layer attractive Hubbard model, New J. Phys. **16**, 013004 (2014).

[6] P. M. Dee, S. Johnston, and T. A. Maier, Enhancing T_c in a composite superconductor/metal bilayer system: A dynamical cluster approximation study, Phys. Rev. B **105**, 214502 (2022).

[7] Y. Zhang, P. M. Dee, B. Cohen-Stead, T. A. Maier, S. Johnston, and R. Scalettar, Optimizing the critical temperature and superfluid density of a metal-superconductor bilayer, Phys. Rev. B **112**, 064510 (2025).

[8] O. Yuli, I. Asulin, O. Millo, D. Orgad, L. Iomin, and G. Koren, Enhancement of the superconducting transition temperature of $La_{2-x}Sr_xCuO_4$ bilayers: role of pairing and phase stiffness, Phys. Rev. Lett. **101**, 057005 (2008).

[9] D. Huang and J. E. Hoffman, Monolayer FeSe on $SrTiO_3$, Annu. Rev. Condens. Matter Phys. **8**, 311 (2017).

[10] M. A. Cazalilla, F. Sols, and F. Guinea, Dissipation-driven quantum phase transitions in a Tomonaga-Luttinger liquid electrostatically coupled to a metallic gate, Phys. Rev. Lett. **97**, 076401 (2006).

[11] A. M. Lobos, A. Iucci, M. Müller, and T. Giamarchi, Dissipation-driven phase transitions in superconducting wires, Phys. Rev. B **80**, 214515 (2009).

[12] See Supplemental Material at http://link.aps.org/supplemental/10.1103/1szk-xwh1 for details on size- and t_{perp}-dependence, simulation hyperparameters and the proximity effect.

[13] U. Schollwöck, The density-matrix renormalization group in the age of matrix product states, Ann. Phys. (NY) **326**, 96 (2011).

[14] F. F. Assaad, M. Bercx, F. Goth, A. Götz, J. S. Hofmann, E. Huffman, Z. Liu, F. P. Toldin, J. S. E. Portela, and J. Schwab, The ALF (Algorithms for Lattice Fermions) project release 2.4. Documentation for the auxiliary-field quantum Monte Carlo code, SciPost Phys. Codebases 1-v2.4 (2025).

[15] F. F. Assaad, M. Bercx, F. Goth, A. Götz, J. S. Hofmann, E. Huffman, Z. Liu, F. P. Toldin, J. S. E. Portela, and J. Schwab, Codebase release 2.4 for ALF (Algorithms for Lattice Fermions), SciPost Phys. Codebases 1-r2.4 (2025).

[16] T. Giamarchi, *Quantum Physics in One Dimension* (Oxford University Press, Oxford, UK, 2003).

[17] E. Gull, A. J. Millis, A. I. Lichtenstein, A. N. Rubtsov, M. Troyer, and P. Werner, Continuous-time Monte Carlo methods for quantum impurity models, Rev. Mod. Phys. **83**, 349 (2011).

[18] G. Bollmark, T. Köhler, L. Pizzino, Y. Yang, J. S. Hofmann, H. Shi, S. Zhang, T. Giamarchi, and A. Kantian, Solving 2D

and 3D lattice models of correlated fermions–combining matrix product states with mean-field theory, Phys. Rev. X **13**, 011039 (2023).

[19] A. Kantian, A. J. Daley, and P. Zoller, η condensate of fermionic atom pairs via adiabatic state preparation, Phys. Rev. Lett. **104**, 240406 (2010).

[20] S. Hirthe, T. Chalopin, D. Bourgund, P. Bojović, A. Bohrdt, E. Demler, F. Grusdt, I. Bloch, and T. A. Hilker, Magnetically mediated hole pairing in fermionic ladders of ultracold atoms, Nature (London) **613**, 463 (2023).